Sādhanā (2020)45:117
https://doi.org/10.1007/s12046-020-01363-9

Theoretical and experimental study on one dimensional fracture grouting in soil medium

ZHENG ZHUO* and LIU RENTAI

Geotechnical and Structural Engineering Research Center, Shandong University, No. 17923, Jingshi Road, Jinan 250061, Shandong, China
e-mail: 413708318@qq.com; rentailiu@163.com

MS received 17 June 2019; revised 20 November 2019; accepted 14 February 2020

Abstract. In this study, a theoretical model of one dimensional fracture grouting in soil is proposed based on fluid mechanics and force analysis during grout fracturing process. Solutions for grout pressure, and the length and width of the fracture are obtained, and the influence of the yield strength on the fracturing behavior is analyzed. Results show that, the grouting distance decreases and the fracture height increases as the yield strength of grout increases. A laboratory test was carried out in this study to validate the proposed theoretical model. The dimension of the solidified grout was measured after excavation. For higher yield strength, the grout front has a blunt shape, which means the pushing effect plays a more important role than the fracturing effect and the fracturing process was controlled by different mechanisms for different yield strength during the experiment. Comparison between the theoretical and the experimental results shows that the proposed model can effectively describe the fracture grouting process.

Keywords. Fracture grouting; laboratory test; fracture shape; grouting pressure.

1. Introduction

Grouting has been used as an effective method of problematic geology treatment for construction of underground project [1–4]. During the grouting process, grout materials are injected into the stratum to fill the voids and provide cohesive force for the geological masses. Thus, the mechanical property of the stratum is improved, which provide sufficient strength for excavation.

In a grouting work, the diffusion mode can be divided into three types: permeation grouting, fracture grouting, and a combination of these two types, which is determined by both the type of grout and the composition of the medium. For chemical solution with Newton fluid behavior, the diffusion mode is always permeation, as the solute can easily penetrate through the pore voids along with water. However, in most cases cement-based grout is preferred, since it has a higher mechanical strength after solidification and a lower cost. Cement-based grout is a typical suspension and is regarded as Bingham fluid. It contains a large amount of cement particles and has much higher viscosity than water. Thus, it is much more difficult for grout suspension to penetrate through pore voids of the stratum. The diffusion mode is mainly determined by the relative magnitude of the pore voids compared with the particle size in the suspension. With pore voids decreasing, the diffusion mode gradually transforms from permeating to fracturing. For clay medium, pore voids are even smaller than the cement particles. The grout suspension can only fracture the soil but hardly penetrate into the pore voids. Therefore, for stratum with low permeability, fracture grouting is the most common flow pattern.

Fracture grouting in soil includes two processes. Firstly, the soil is fractured due to grouting pressure. Then, the grout spreads to further distance as the fracture propagates. The pressure at which fracture occurs is called initiation pressure. The initiation pressure depends on various parameters, such as the initial circumferential stress, the Poisson's ratio of the soil skeleton, and the degree of saturation and consolidation. The hydraulic fracturing mechanism has been extensively studied by field excavation and laboratory tests [5–9]. Lo and Kaniaru [10] concluded that the pressure increases with the decrease of water content and the increase of consolidation. Other studies also showed the influence of the saturate state on the fracturing behavior by comparing difference of hydraulic fractures in both partially saturated and fully saturated clays [11–13]. However, the process of fracture propagation can hardly be observed directly, and the information about the fracture shape and pressure variation is acquired usually by indirect measurements.

In recent years, a series of empirical and theoretical models has been proposed for estimating the initiation pressure, and the length and thickness of the fracture [14–17]. However, the validation and the application

*For correspondence
Published online: 11 May 2020

conditions of these models still need to investigate. In this study, a theoretical model of one dimensional fracture grouting in soil is proposed based on fluid mechanics and force analysis during grout fracturing process. The fracture shape is determined based on the boundary conditions. Solutions for grout pressure, and the length and width of the fracture are obtained, and the influence of the yield strength on the fracturing behavior is analyzed. A laboratory test was carried out in this study to validate the proposed theoretical model. Soil was filled into a container which is 1 m long. Then, grout suspension was injected into the container to fracture the soil. The dimension of the solidified grout was measured after excavation. Comparison between the theoretical and the experimental results shows that the proposed model can effectively describe the fracture grouting process.

2. A theoretical model of fracture grouting

2.1 *Fracture shape*

The fracture shape depends on the boundary conditions during grouting process. Generally, the fracture shape can be divided into three types: plate, radial plate and tube. With the information of the fracture shape, the variation of fracture length and thickness with different grouting volume can be calculated (figure 1).

For the shape of a plate, the equilibrium equation is written as:

$$\Delta p \cdot w \cdot h = 2\xi\tau \cdot w \cdot l \tag{1}$$

where l, w and h are the length, width and height of the fracture, respectively. TheΔp is the injection pressure reduced by the minimum pressure for fracturing, τ is the shear stress of the grout, and ξ is a correction factor which accounts for the tortuosity of the fracture. By simplifying Eq. (1), the ratio between the length and the height of the fracture can be written as:

$$\frac{l}{h} = \frac{\Delta p}{2\xi\tau} \tag{2}$$

The total injection volume V is expressed as:

$$V = h \cdot w \cdot l \tag{3}$$

Substituting Eq. (3) into Eq. (2) yields the solution of length and height as a function of grouting volume:

$$l = \sqrt{\frac{\Delta p}{2\xi\tau} \cdot \frac{V}{w}}, \quad h = \sqrt{\frac{2\xi\tau}{\Delta p} \cdot \frac{V}{w}} \tag{4}$$

2.2 *Grouting pressure and velocity*

Cement grout is usually considered as a Bingham fluid, whose rheological behavior is either like a rigid solid or a viscous fluid. The constitutive relationship is expressed as Eq. (5), where τ_0 is the yield strength, μ is the grout viscosity and $\dot{\gamma}$ is the shearing rate.

$$\tau = \tau_0 + \mu\dot{\gamma} \tag{5}$$

From the Bingham model it follows that the grout does not move unless the shear stress exceed the yield strength. During grout advancing process, the grout in the fracture is divided into three layers: an upper and a lower boundary layers and a stiff core with a thickness of δ, which is expressed as

$$\delta = \tau\left|\frac{\mathrm{d}p}{\mathrm{d}x}\right|^{-1}, \quad \delta < \frac{h}{2} \tag{6}$$

The velocity distribution along y axis is expressed as:

$$v = \begin{cases} \frac{1}{\mu}\left(-\frac{h^2-4y^2}{8} \cdot \frac{\mathrm{d}p}{\mathrm{d}x} - \tau_0 \cdot \frac{h-|y|}{2}\right), & \left(\frac{\delta}{2} < |y| < \frac{h}{2}\right) \\ \frac{1}{\mu}\left(-\frac{h^2-\delta^2}{8} \cdot \frac{\mathrm{d}p}{\mathrm{d}x} - \tau_0 \cdot \frac{h-|\delta|}{2}\right), & \left(|y| \le \frac{\delta}{2}\right) \end{cases} \tag{7}$$

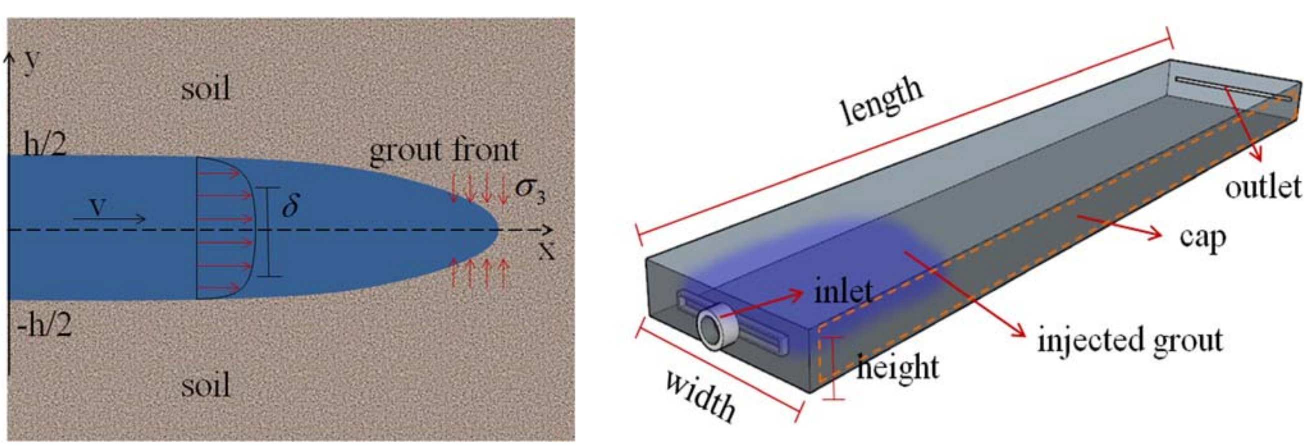

Figure 1. Theoretical model of fracture grouting and the flowing pattern in the container of the experiment.

The average value of velocity is expressed as:

$$\bar{v} = \frac{1}{h}\int_{-h/2}^{h/2} v\mathrm{d}y \tag{8}$$

For a constant injection rate condition, the relationship between injection rate and the velocity is expressed as:

$$\bar{v} = \frac{q}{hw} \tag{9}$$

Substituting Eq. (7) and Eq. (9) into Eq. (8) yields:

$$\frac{q}{hw} = \frac{\mathrm{d}p}{\mathrm{d}x} \cdot \frac{h^2}{12\mu}\left(1 - 3\frac{\delta}{h} + 4\frac{\delta^3}{h^3}\right) \tag{10}$$

During the fracturing process, the injection pressure is usually very high, thus the stiff core is much small than the height of the fracture. The three-cubed term of the ratio parenthesis can be neglected. Then, the expression of p along x axis can be easily obtained by integration:

$$p = \left(\frac{12\mu q}{h^3 w} + 3\tau\right)x + C \quad x \le l \tag{11}$$

where C is an integration constant. According to the fracturing condition, C equals the fracture initiation pressure. Equation (10) is modified as:

$$p = \left(\frac{12\mu q}{h^3 w} + 3\tau\right)x + \sigma_3 \quad x \le l \tag{12}$$

Equations (3), (4) and (11) give the solution for grouting pressure, grout length and height during fracture grouting process.

3. Experiment setup

In order to validate the proposed theoretical model, a laboratory experiment was conducted to investigate the fracturing behavior of grout suspension and the shape of grout vein after solidification. The procedures of the grout fracturing experiments included the following steps: preparation of the soil specimen, grout injection, waiting while the grout solidifies, and the excavation of the soil. A schematic view of the general procedures of the experiment is shown in figure 2. It should be noticed that in a real grouting work the geological condition would be much more complex, and the flow pattern of grout suspension could vary a lot depending on the real conditions. However, a real engineering background is not considered in the experiment. Flow of grout suspension was restricted to one-dimension, which is in accordance with the assumptions adopted in the theoretical model. The influence of gravity is also neglected, since it is insignificant compared with the injection pressure. Therefore, the container for grout injection was set up horizontally for convenience of operation.

The soil was obtained locally in the field of quaternary formation. It contains about 50% silt, 20% clay, and 30% other minerals. The grain size distribution curve is shown in figure 3. The distribution curve covers a wide range, which indicates that the soil medium has a good gradation. The coefficient of curvature and coefficient of non-uniformity were also calculated. The values are 123.5 and 16.7, respectively. Specific gravity, void ratio, and other physical properties were measured according to the standard of American Society for Testing and Materials (ASTM). These parameters are listed in table 1.

Firstly, soil was oven-dried at 120°C for one day before being used. Then the soil was filled into a rectangular container, with a dimension of 1 m long, 0.2 m wide and

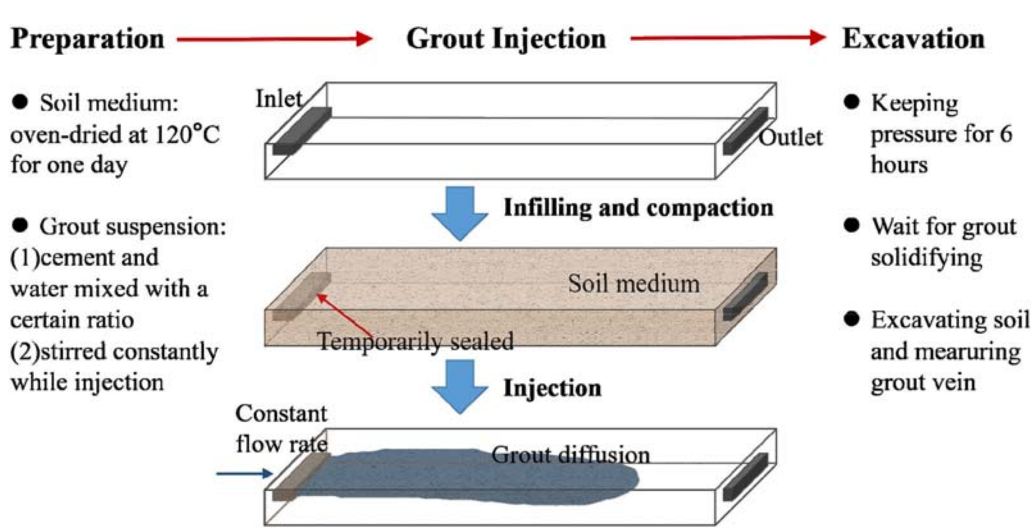

Figure 2. General procedures for the experiment of hydraulic fracturing with grout suspension.

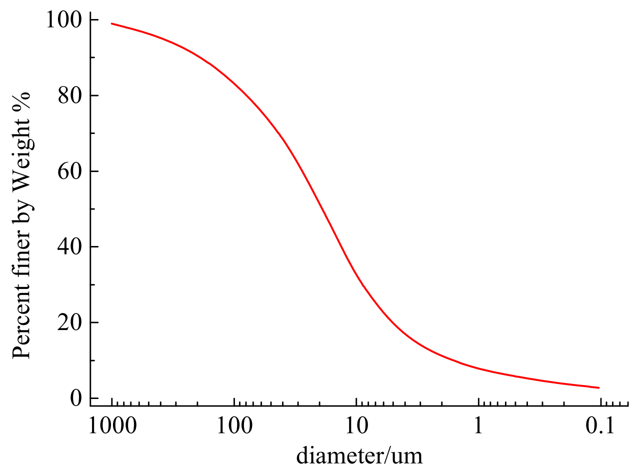

Figure 3. Grain size distribution of the soil medium.

0.05 m high. The filling amount of the soil was controlled by the target degree of density and compactness. However, the degree of compaction should not be too high, in case there was no space for grout suspension to be injected. An injection inlet was mounted at one end of the container which was used for grout injection. At the other end of the container, there was an outflow hole. Water and grout suspension could flow out of the hole but the soil was restricted in the container. The inlet and outlet were temporarily sealed during the soil filling process in case the soil entered the tubing and clog it.

After preparation, the experimental setup was assembled and confining pressure was applied on the lateral sides of the container. Then, grout was injected by a pump with a constant flow rate. The water–cement ratio was altered in order to see the influence on the hydraulic fracturing behavior. During injection, the grout suspension was being stirred constantly in case of sediment (figure 4).

Table 2. Parameters of the grout fracturing experiment.

Name	Unit	Symbol	Value
Viscosity	Pa.s	μ	0.1
Yield strength	Pa	τ	$1\sim5$
Grouting time	s	t	60
Pumping rate	ml/s	q	10

After injection, the container was kept with the final pressure for 6 h before it was disassembled. This allowed the grout suspension to solidify inside the specimen while maintaining the shape of the space which the grout suspension occupied. Afterwards, soil was excavated out of the container to examine the shape of the grout rigid body. The length and width of the grout was measured according to different grouting condition. During injection, the pumping rate was controlled at 10 ml per second. The injection process ceased after grouting for 60 s, or grout suspension reached the outlet of the container. The experimental parameters mainly used in this study are shown in table 2.

4. Results and analysis

The final grout distance and height were measured after excavation of soil. Figure 5 shows comparison of theoretical value and experimental value of grout distance and height according to different yield strength of grout, after

Table 1. Physical properties of the soil.

Name Unit	Dry density g/cm^3	Void ratio –	Porosity –	Specific gravity –	Repose angle deg
Maximum value	1.35	1.25	0.54	2.3	43
Minimum value	1.06	0.70	0.41		

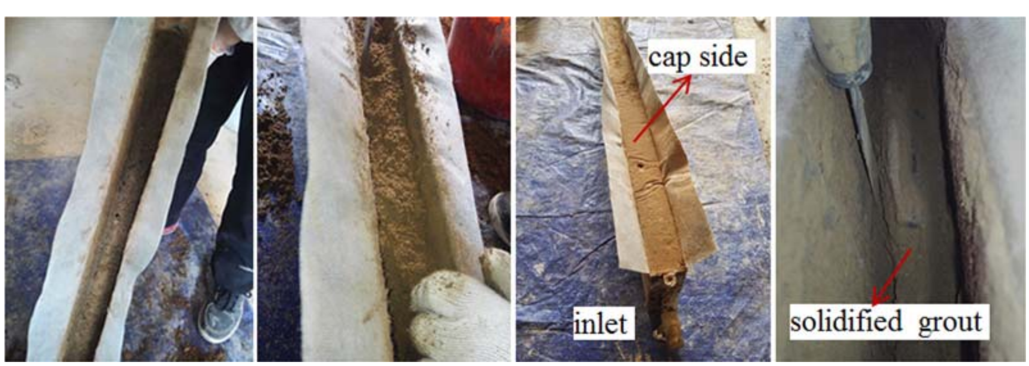

Figure 4. Experiment procedure and excavation results of the grout fracture.

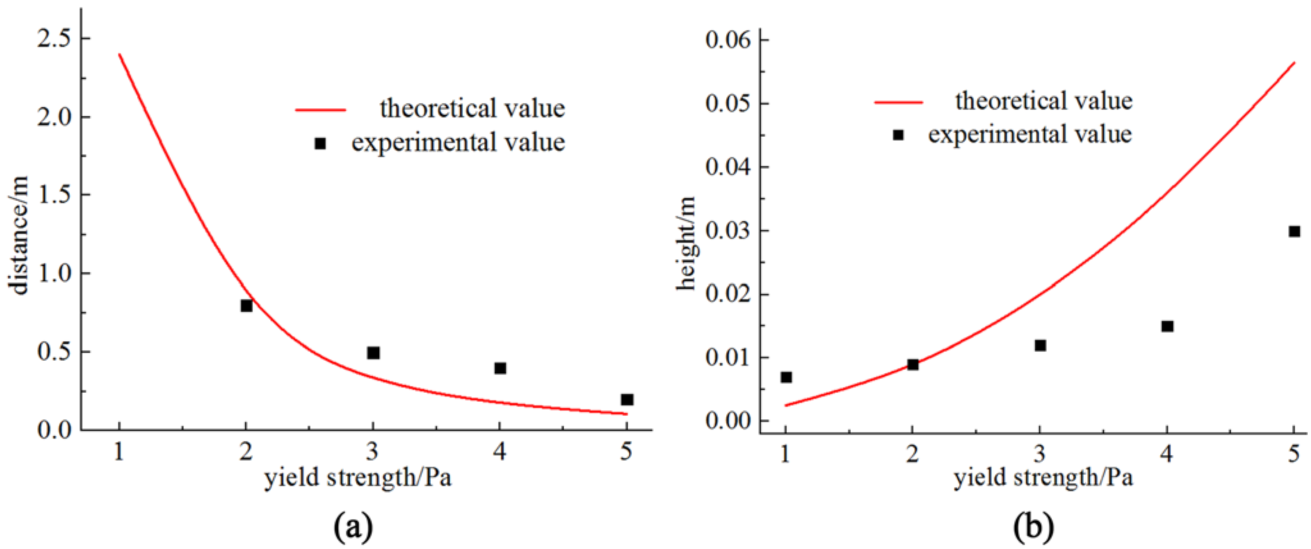

Figure 5. Variation of grout distance and grout height with different yield strength.

grouting for 60 s. It should be noticed that the grout height and width is not constant along the grout advancing direction, and these experimental values are acquired by averaging measurements at different distance from the injection hole. The experimental value of grouting distance with yield strength of 1 Pa is absent because the grout reached the outlet but the grouting time was less than 60 s, and the injection ceased. From the red line, which represents the theoretical value, it can be seen that the final grouting distance decreases as the yield strength of grout increases. Moreover, the decreasing rate is nonlinear. The decreasing rate is very high at first and then becomes relatively low. This is because as the yield strength increases, the grout becomes thicker, and moves more like a rigid body. The fracturing ability reduces during the injection process. Instead, grout can only push the soil forward, and bears more resistance, which prevent grout from reaching further distance. The relationship between grouting distance and the yield strength according to the experimental result shows a similar trend with that from theoretical results, except the nonlinearity is not very obvious. In general, the theoretical and experiment values are very close, which means that the theoretical model proposed in this study is reasonable.

Figure 5b shows the relationship between the height of the grout fracture and the yield strength. As can be seen, the fracture height increases with the increase of the yield strength. The increasing rate is comparatively low at first and then becomes higher. The increasing rate of the experimental result is lower compared with that of theoretical result. This is because that the proposed theoretical model in this study has neglected the influence of pressure-induced filtration effect, which lowers the fluidity of grout and leads to difficulty for grout injection. From the experimental value, it can be seen that the fracture height varies in a range between 0.007 m and 0.015 m, while the yield strength is less than 4 Pa. The variation is very small, which means the fracturing behavior was similar during the injection process. However, for the yield strength of 5 Pa, the fracture height rises to 0.03 m, which is obviously

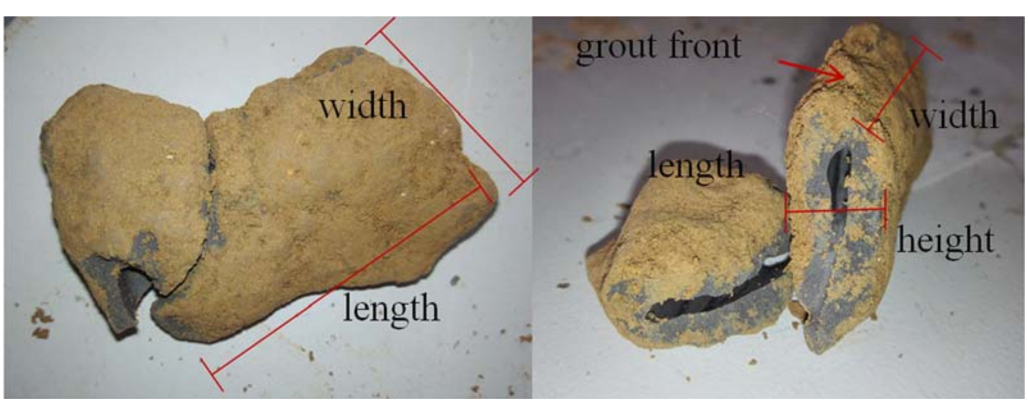

Figure 6. Solidified grout after excavation.

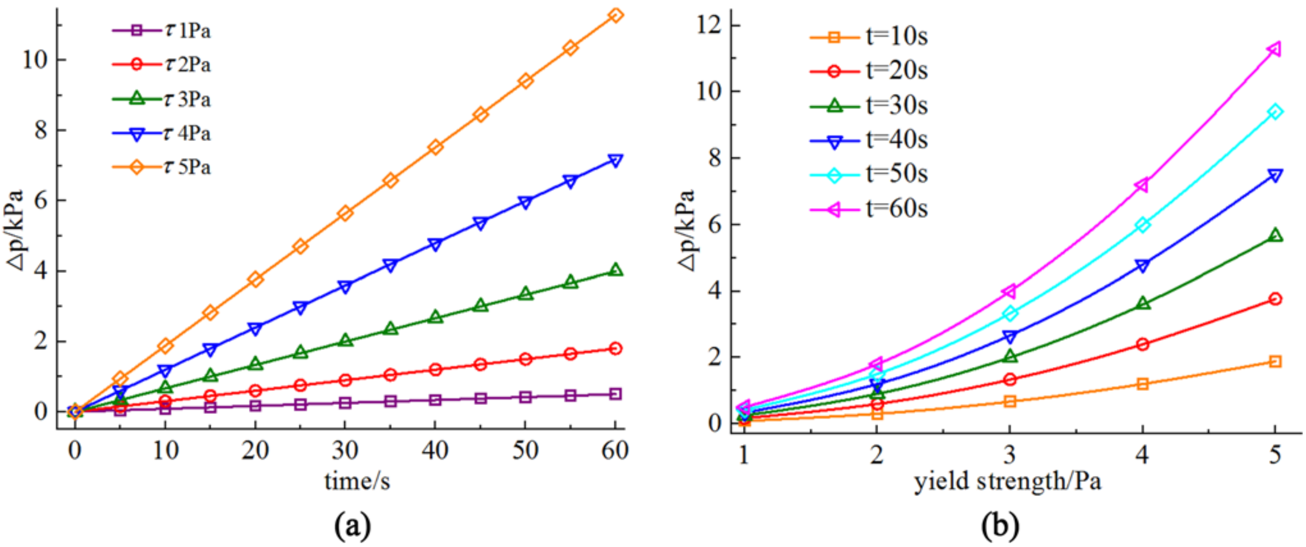

Figure 7. Variation of grout pressure with different times and yield strength.

higher than the other results. A possible explanation is that the fracturing process was controlled by a different mechanism. Figure 5a shows that the grout distance was only about 0.2 m for this case. The excavation of the solidified grout is shown in figure 6. As can be seen, the grout front has a blunt shape. In this case, the pushing effect plays a more important role than the fracturing effect. The pushing behavior needs to overcome a larger resistance than fracturing, since the soil becomes more and more compacted as the grout moves forward. Thus, it can be concluded that the yield strength of the grout suspension should not be too height so that it can fracture soil effectively.

Figure 7 shows the variation of grouting pressure at different times and different yield strength of grout according to the theoretical results. As can be seen from figure 7a the grouting pressure increases linearly as time increases. The increasing rate of grouting pressure is the lowest when the yield strength is 1 Pa and is the highest when the yield strength is 5 Pa. This is because that when the yield strength is low, the grout suspension is easy to move and the pressure loss is small. As the yield strength increases, the grout suspension losses its fluidity and is harder to move. Figure 7b shows the relationship between grouting pressure and yield strength at certain times. It can be seen that the grouting pressure increases nonlinearly with yield strength. The increasing rate is slow at first and then becomes higher. Moreover, the nonlinearity is more obvious as the time increases. This is because as time

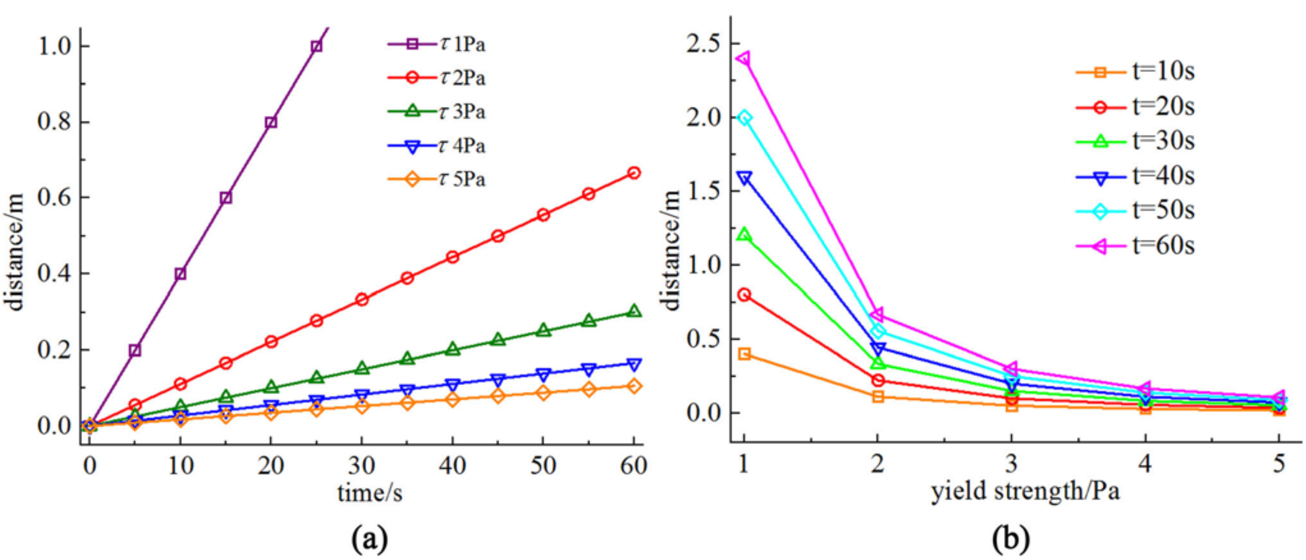

Figure 8. Variation of grouting distance with different times and yield strength.

increases, the grouting length becomes longer and the contact area between the grout and the soil is larger, leading to a higher resistance from soil. At grouting time of 60 s, the difference of grouting pressure becomes very large. For yield strength of 1 Pa, the grouting pressure at 60 s is no more than 1 kPa, while for yield strength of 5 Pa, the grouting pressure reaches 12 kPa. For an engineering project, the grouting pressure should not be too high in case of engineering accident. Thus, the grout property should be carefully chosen in order to achieve an effective grouting result.

Figure 8 shows the variation of grouting distance with different times and yield strength. As can be seen from figure 8a, the grouting distance increases linearly with time. When the yield strength is small, the increasing rate is high. On the opposite, when the yield strength is large, the increasing rate is high. Figure 8b shows the relationship between the grout distance and yield strength at different times. As can be seen, the grouting distance decreases nonlinearly with the yield strength. The decreasing rate is high at first and then becomes lower. It should be noticed that the calculation results with yield strength of 1 Pa exceeded the range of the experimental results, and the reliability is not convinced. The extreme grouting distance was restricted at 1 m during the experiment but the calculated grouting distance with yield strength of 1 Pa reaches 2.5 m at 60 s. For grouting distance less than 1 m, the calculation and experimental results are similar. This means that the proposed theoretical model in this study has a range of application. Calculation for a longer grouting distance needs further study.

5. Conclusion

In this paper, a theoretical model of one dimensional fracture grouting in soil is proposed based on fluid mechanics and force analysis during grout fracturing process. A laboratory test was carried out to validate the proposed theoretical model. Solutions for grout pressure, and the length and width of the fracture are obtained. The main conclusions are as follows:

The fracture length was negatively correlated with the yield strength of grout suspension. As the yield strength increased from 1 Pa to 2 Pa, the diffusion distance decreased drastically. However, the decreasing rate turned to be moderate when the yield strength continued to increase. This indicates that the fracturing ability of grout suspension is sensitive to the yield strength. The shape of the fracture would be thicker for grout with a higher yield strength. In this case, grout can only push the soil forward and it moves more like a rigid body. Insufficiency of fracturing ability would cause higher resistance for grout suspension, which prevents grout from reaching further distance.

The fracture height was positively correlated to the yield strength of grout suspension, with a steady growth at first followed by a surge when the yield strength was in a higher range. This trend is in accordance with the variation of the fracture length. However, the value of fracture height measured in the experiment was lower compared with the theoretical result. The difference might be induced by the filtration effect, which is not considered in the proposed theoretical model. During the fracturing process, some of the water was pressed out of the grout and into the soil during injection, which caused mass loss of grout. However, the leakage of water was eliminated since a thin impermeable filter cake composed of cement particles gradually formed on the fracture surface, which stopped the following water from being pressed out of the grout and flowing into soil medium.

The difference of the shapes of fracture front observed from the experiment indicates that there were different mechanisms dominating the fracturing process. For higher yield strength, the grout front had a blunt shape, which means the pushing effect played a more important role than the fracturing effect. According to the experiment result, fracture height varied in a range between 0.007 m and 0.015 m while the yield strength was less than 4 Pa. For a yield strength of 5 Pa, fracture height rose to 0.03 m. This could significantly affect the stress state and failure mode of the surrounding soil at the fracture tip. Therefore, in a practical grouting work, the yield strength of the grout suspension should not be too height so that it can fracture soil effectively.

Acknowledgement

This work was financially supported by General Program of National Natural Science Foundation of China (51779133), National Key R&D Plan of China (2016YFC0801604) and Joint Funds of National Natural Science Foundation of China (U1706223).

References

[1] Yun J-W, Park J-J, Kwon Y-S et al 2017 Cement-based fracture grouting phenomenon of weathered granite soil. *KSCE Journal of Civil Engineering* 21(1): 232–242

[2] Zhang X, Li S, Zhang Q et al 2010 Filed test of comprehensive treatment method for high pressure dynamic grouting. *Journal of China Coal Society* 35(08): 1314–1318 (**in Chinese**)

[3] Ruan W-J 2005 Spreading model of grouting in rock mass fissures based on time-dependent behavior of viscosity of cement-based grouts. *Chinese Journal of Rock Mechanics and Engineering* 24(15): 2709–2714 (**in Chinese**)

[4] Li S, Liu R, Zhang Q et al 2013 Research on C-S slurry diffusion mechanism with time-dependent behavior of

viscosity. *Chinese Journal of Rock Mechanics and Engineering* 32(12): 2415–2421 (**in Chinese**)

[5] Murdoch L C 1990 A field test of hydraulic fracturing in glacial till. In: *Proc 15th an Res Symp, Ohio, 600/9-90-006*. Cincinnati: US Environmental Protection Agency. p. 164–174.

[6] Warninski N R 1983 Investigation of the accuracy and reliability of in-situ stress measurements using hydraulic fracturing in perforated cased holes. In: *Proc. 24th US Symp Rock Mech, Golden*, pp. 773–786

[7] Northrop D A, Warpinski N R, Schmidt R A and Smith C W 1978 Stimulation and mine back experiment project: the direct observation of hydraulic and explosive fracturing tests. In: *Proc. Symp. Enhanced Oil & Gas Recovery & Improved Drilling Methods, Tulsa*; pp. l–14.

[8] Kleinlugtenbelt R, Bezuijen A and van Tol A F 2006 Model tests on compensation grouting. *Tunn Undergr Sp Technol* 21: 435–436

[9] Barsoum R 1976 Furthur application of quadratic isoparametric elements to linear fracture mechanics of plate bending and general shells. *International Journal for Numerical Methods in Engineering* 11: 167–169.

[10] Lo K Y and Kaniare K 1990 Hydraulic fracture in earth and rock-fill dams, Canada *Geotechiques* 27: 496–506.

[11] Soga K, Au S K A, Jafari M R and Bolton M D 2004 Laboratory investigation of multiple grout injections into clay. *Geotechnique* 54(2): 81–90

[12] Mori A and Tamura M 1987 Hydro-fracturing pressure of cohesive soils. *Soils and Foundations, Japanese Society of Soil Mechanics and Foundation Engineering* 27(1): 14–22

[13] Murdoch L C 1990 A field test of hydraulic fracturing in glacial till, In: *Proceedings of the 15th Annual Reservoir Symposium, Cincinnati, Ohio. 600/9-90-006*, Washington, DC: US Environmental Protection Agency, 164–174

[14] Li S-C, Zhang W-J, Zhang Q-S et al 2014 Research on advantage-fracture grouting mechanism and controlled grouting method in water-rich fault zone. *Rock and Soil Mechanics* 35(3): 745–751 (**in Chinese**)

[15] Chen T-L, Zhang L-Y and Zhang D-L 2014 An FEM/VOF hybrid formulation for fracture grouting modeling. *Computers and Geotechnics* 58: 14–27

[16] Li P, Zhang Q-S, Zhang X et al 2014 Analysis of fracture grouting mechanism based on model test. *Rock and Soil Mechanics* 35(11): 3221–3230 (**in Chinese**)

[17] Zou J-F, Tong W-Q, Luo H et al 2013 Mechanism of fracture grouting for fractured rock based on Hoek–Brown failure criterion. *Journal of Central South University (Science and Technology)* 7: 2889–2896 (**in Chinese**)